Taccone, Florent; Antoine, Germain; Goutal, Nicole; Delestre, Olivier

Improving TELEMAC on a simple test case to simulate runoff and erosion generation

Improving TELEMAC on a simple test case to simulate runoff and erosion generation

Florent Taccone,
Germain Antoine
and Nicole Goutal
Laboratoire National d'Hydraulique et Environnement, EDF R&D
Laboratoire d'Hydraulique Saint-Venant
6 Quai Watier 78400 Chatou France
Email: florent.taccone@gmail.com

Olivier Delestre
Laboratoire de Mathématiques J.A. Dieudonné
UMR 7351
École Polytech Nice-Sophia
Université de Nice-Sophia Antipolis
Parc Valrose 06108 Nice France

***Abstract*—This paper focuses on how to ensure the robustness of the resolution of Shallow Water Equations in the TELEMAC2D computation code in the case of rain induced runoff on steep slopes. To reproduce these conditions, a straight channel with a variable slope on which drops a constant rain is defined. With this test case, a comparison between the simulated discharge at the outlet and an analytical solution of the Shallow Water Equations for the rising part of the hydrograph and the plateau has been done. By stopping the rain in the middle of a simulation, numerical results and an analytical solution of the kinematic wave approximation were confronted during the emptying of the domain.**

Limitations of the numerical resolution are highlighted with the finite volume schemes. Improvements were made to better represent the rainfall-runoff responses, like another method of hydrostatic reconstruction [7] which has been implemented. Then, the model is extended to pollutant transfers and sediment transport in suspension. These results provide a strong basis for future application of modeling erosion at the watershed scale.

I. Introduction

The sediment transfers at the watershed scale involve several processes, because of the heterogeneity of the soil, but also the different flow regimes due to the complex topography of the field and the time and space variability of the meteorological conditions. In the mountainous regions, the filling of reservoirs is an important issue in terms of efficiency and environmental acceptability for producing hydro-electricity. Thus, the modelling of the sediment tranfers on highly erodible watershed is a key challenge from both economic and scientific points of view. A physically-based representation provides an explicit representation of the hydraulic and sedimentary variables, but needs several parameters and a fine discretization of the domain. The erosion processes being heavily reliant on the flow characteristics, we must have a robust and accurate representation of hydraulic dynamics. A simple test case has been defined in order to evaluate the different resolution methods of the Shallow Water equations with TELEMAC2D, in the particular case of steep slopes and shallow water depths.

One of the main difficulties is to have a numerical scheme able to represent correctly the hydraulic transfers, preserving the positivity of the water depths, dealing with the wet/dry interface and being well-balanced (in the sense of [13]) meaning preserving the hydrostatic balance of a lake at rest. Few schemes verifying these properties exist, and their accuracy still need to be evaluated in the case of rain induced runoff on steep slopes. Moreover, it is necessary to represent the suspension of tracers and sediments in the flow, from the hillslopes to the outlet of the watershed, with as little dispersion as possible in supercritical flow. In TELEMAC2D, several advection schemes have been recently implemented ([15] and [14]) to overcome this problem for river flow applications and need to be tested for runoff simulations. Subsequently, it is important to figure out the mesh and the hydraulic scheme effects on the erosion generation to anticipate the scaling effect for a real watershed application.

In this paper, a straight channel test case, with a variable slope, on which drops a steady rain is used, which represents what can be observed in a mountain watershed context. Different finite volume schemes are analyzed, and more particularly their bottom source term discretization. Then, the advection of passive tracer is tested in this situation to evaluate its efficiency. Finally, SISYPHE is used to represent the soil erosion on the test case and a study of the effect of the hydraulic scheme on rill generation has been realized.

II. Materials and Methods

In this work, the simulations have been performed with the V7P1R1 version of TELEMAC2D and SISYPHE.

A. Presentation of the test case

Following the work of [16], a test case on a straight channel of dimensions 4.04 X 0.115 m is created. On this domain, a steady rain, with an intensity of 25 mm/h, is applied during 100 s. The discharge at the outlet of this channel is observed. The duration of the simulation is 200 s, the first 100 seconds describing the rise of the hydrograph and the constant value and the last 100 seconds the emptying of the domain. The spatial discretization of the channel is a triangular mesh with a length of 1 cm. The choice of this test has been motivated by the fact that [9] gives analytical solutions for the discharge. To avoid effects of the upstream wall boundary, a 5 meters channel is created and the rain starts to fall 0.96 m away.

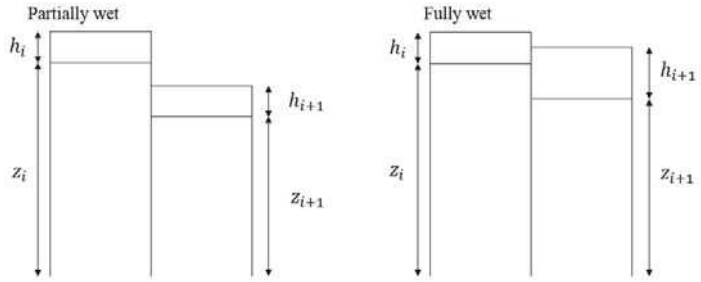

Fig. 1: Illustration of the partially wet and fully wet regimes at the interface of two cells

B. Overland flow simulation

To simulate rain induced runoff, TELEMAC2D solves the Shallow Water equations which are:

$$\frac{\partial U}{\partial t} + \frac{\partial F(U)}{\partial x} = S, \tag{1}$$

where $U = (h, hu)$, $F(U) = (hu, hu^2 + gh^2/2)$ and $S = (R, -gh(\partial_x z + S_f))$ with h the water height in m, u the flow velocity in m/s, g the gravity constant in m/s^2, R the rain intensity in m/s, z the bottom elevation in m and S_f the friction slope. For that, the following explicit finite volume scheme is used:

$$U_i^{t+1} = U_i^t - \frac{\Delta t}{\Delta x}(F_{i+1/2}^t - F_{i-1/2}^t) + \frac{\Delta t}{\Delta x} S_i, \tag{2}$$

where $F_{i+1/2}^t = F(U_{i+1/2+}, U_{i+1/2-})$ is the numerical flux at interface $i+1/2$ and $S_i = (R_i, s_{i+1/2-} + s_{i-1/2+})$ are the source terms. The friction slope is added to the scheme (2) by a semi-implicit treatment (see [12], [5] and [10]). It follows a Chézy's law where the coefficient is set to 30 m$^{1/2}$/s in this case.

Concerning the bottom source term discretization, one can use a hydrostatic reconstruction method and define the intermediate states $U_{i-1/2+} = (h_{i-1/2+}, h_{i-1/2+}u_i)$, $U_{i+1/2-} = (h_{i+1/2-}, h_{i+1/2-}u_i)$, $s_{i-1/2+}$ and $s_{i+1/2-}$. The classical hydrostatic reconstruction presented by Audusse *et al.* [1] gives:

$$\begin{aligned} h_{i-1/2+} &= \max(h_i + z_i - \max(z_{i-1}, z_i), 0), \\ s_{i-1/2+} &= \tfrac{g}{2}(h_i^2 - h_{i-1/2+}^2), \\ h_{i+1/2-} &= \max(h_i + z_i - \max(z_i, z_{i+1}), 0), \\ s_{i+1/2-} &= \tfrac{g}{2}(h_{i+1/2-}^2 - h_i^2), \end{aligned}$$

while a new reconstruction method introduced by Chen and Noelle [7] gives:

$$\begin{aligned} z_{i+1/2} &= \min(\max(z_i, z_{i+1}), \min(h_i + z_i, h_{i+1} + z_{i+1})) \\ h_{i-1/2+} &= \min(h_i + z_i - z_{i-1/2}, h_i), \\ s_{i-1/2+} &= \tfrac{g}{2}(h_i - h_{i-1/2+})(z_{i-1/2} - z_i), \\ h_{i+1/2-} &= \min(h_i + z_i - z_{i+1/2}, h_i), \\ s_{i+1/2-} &= \tfrac{g}{2}(h_i + h_{i+1/2-})(z_i - z_{i+1/2}). \end{aligned}$$

Based on the definition given by [7], a fully wet and a partially wet regime are distinguished at the interface of two cells. The figure 1 illustrates these regimes. The Audusse *et al.* [1] and Chen and Noelle's [7] hydrostatic reconstruction are computing exactly the same source term for the fully wet case. The Chen and Noelle's method modifies the source term in the partially wet case to better take into account the slope effect.

An alternative to the hydrostatic reconstruction, presented by Berthon and Foucher [3], consists in modifying the scheme (2) like:

$$U_i^{t+1} = U_i^t - \frac{\Delta t}{\Delta x}(X_{i+1/2}F_{i+1/2}^t - X_{i-1/2}F_{i-1/2}^t) + \frac{\Delta t}{\Delta x} S_i,$$

with $X_{i+1/2}^k = \begin{cases} \frac{h_i}{h_i + z_i} \text{ if } F_{i+1/2}^t > 0 \\ \frac{h_{i+1}}{h_{i+1} + z_{i+1}} \text{ elsewhere} \end{cases}$. The intermediate states become:

$$\begin{aligned} h_{i-1/2+} = h_{i+1/2-} &= h_i + z_i, \\ s_{i-1/2+} + s_{i+1/2-} &= \tfrac{g}{2} H_{i-1/2} H_{i+1/2} (X_{i+1/2} - X_{i-1/2}) \end{aligned}$$

with $H_{i+1/2}^k = \begin{cases} h_i + z_i \text{ if } F_{i+1/2}^t > 0 \\ h_{i+1} + z_{i+1} \text{ elsewhere} \end{cases}$.

The numerical fluxes are calculated with the HLLC method introduced by [23] and applied to the Shallow Water equations in [22].

C. Analytical solutions

[9] describes analytical solutions of the discharge at the outlet of the domain of the Shallow Water equations (1) for the rising part of the hydrograph and the constant value, and a kinematic wave approximation solution (3) for the complete problem. This approximation writes:

$$\frac{\partial h}{\partial t} + \frac{\partial hu}{\partial x} = P, \ \frac{\partial z}{\partial x} = -S_f \tag{3}$$

and the relative error between solutions of (1) and (3) is inferior to 1% for the rise of the hydrograph and the plateau for a slope superior to 1% on this test case. Using the exact solution of (1) for the 100 first seconds and the exact solution of (3) for the emptying of the domain, it is possible to compare the precision of the schemes.

D. Passive tracer and sediment transport

As described in [21], the suspended sediment transport is governed by the advection equation:

$$\frac{\partial hC}{\partial t} + \frac{\partial huC}{\partial x} = E - D, \tag{4}$$

with C the volumic concentration of sediment in the flow, E the erosion flux in m/s and D the deposition flux in m/s calculated with the classical Krone-Partheniades law with cohesive sediments. In each simulation, the bed is considered uniform, with one class of sediment. To simulate soil erosion with SISYPHE, the following parameters are chosen:

- Partheniades coefficient: 10^{-3} m/s,
- Critical erosion shear stress: 0.05 Pa,
- Critical deposition shear stress: 0.05 Pa,
- Sediment diameter: 40 μm,
- Skin friction coefficient: 1.

The passive tracers are simulated with the continuity equation (4) without source terms. To solve this equation, the LIPS

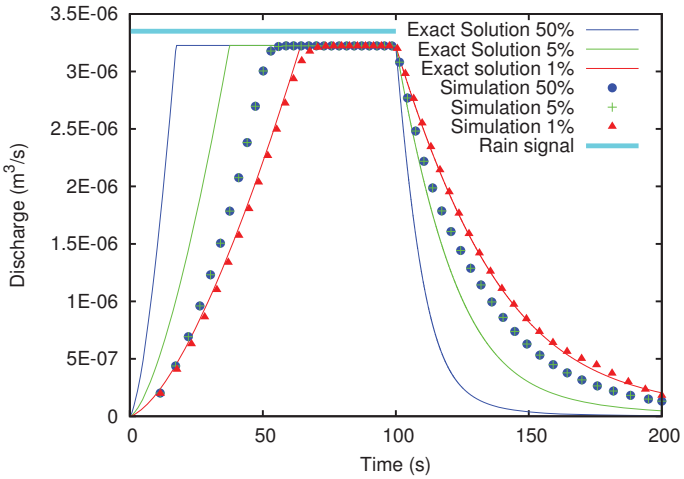

Fig. 2: Discharge (m^3/s) at the outlet of the domain during 200 s, comparison between simulation and analytical solution with the Audusse *et al.* reconstruction [1]

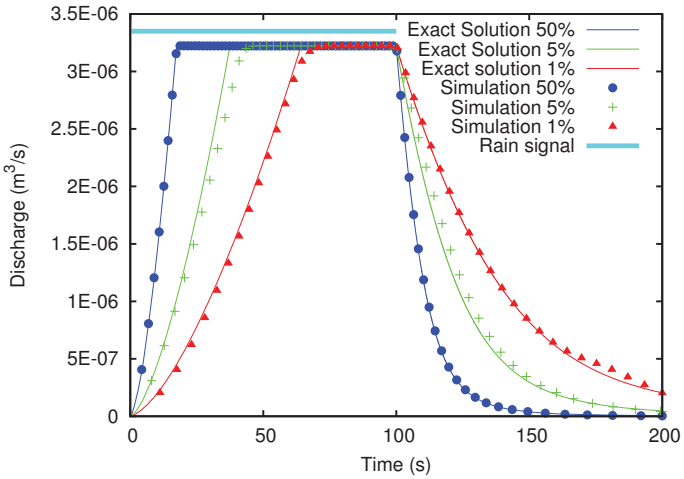

Fig. 3: Discharge (m^3/s) at the outlet of the domain during 200 s, comparison between simulation and analytical solution with the Chen and Noelle's reconstruction [7]

scheme has been used with three corrector steps (see [15]) as well as the ERIA scheme (see [14]), for their ability to deal with vacuum states.

III. Results

A. Hydraulic tranfers

The behaviour of the schemes are compared to the analitycal solution to compare their accuracy in the case of runoff with shallow water depths and steep slopes.

Figure 2 presents the discharge at the outlet with the classical hydrostatic reconstruction (Audusse *et al.* [1]). This scheme presents a limitation for steep slopes. Indeed, the results for the 5% and 50% slopes are identical. Moreover, for the 1% slope simulation, an irregularity is observed during the emptying of the domain after 160 s.

With the Chen and Noelle's [7] hydrostatic reconstruction, the discharges at the outlet are closer to the analitycal solutions. The figure 3 presents these results. This method corrects the slope limitation observed previously. However, there is a lag between the simulation results and the exact solution for the 5% slope and the irregularity at the end of the simulation for the 1% slope is more important.

The third scheme introduced by Berthon and Foucher [3] has been implemented in TELEMAC2D and tested. The figure 4 shows the results of the simulations with this scheme. This method is very efficient to solve the Shallow Water equations in this case. Nevertheless, this scheme has difficulties to treat the dry zones. Indeed, figure 5 shows aberrant velocities at the wet/dry interface with the Berthon and Foucher's scheme [3]. To limit that effect, the fluxes between wet and dry cells has been calculated with the Chen and Noelle's scheme, and this modification improves the treatment of vacuum states, as it is shown in figure 6. This modification improves the results on this test case but does not ensure a better equilibrium of the scheme in other configurations. The figure shows also that the boundary condition accelerates the flow significantly with

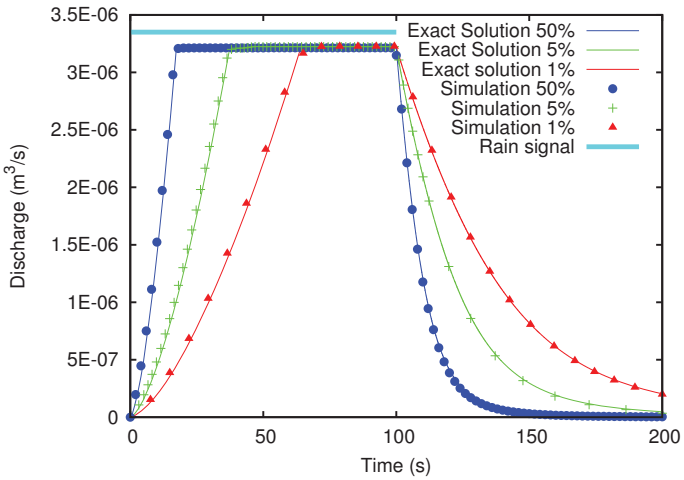

Fig. 4: Discharge (m^3/s) at the outlet of the domain during 200 s, comparison between simulation and analytical solution with the Berthon and Foucher's scheme [3]

the Berthon and Foucher's scheme [3] but it has been tested in every configuration that the downstream boundary does not impact the hydraulic results, shifting it several meters far from the discharge measurement, or creating a break in slope to accelerate the flow at the end of the channel.

To evaluate the precision of each scheme, table I shows the relative error of the computed discharges at the outlet compared with the analytical solution of the shallow water equation during the first 100 second of the simulations. The emptying of the domain is not taken into account because the exact solution of the kinematic wave system (3) is only an approximation of the Shallow water equations (1) solved numerically. The error is calculated by comparing the simulated value of the discharge q_s and the exact solution q_e at each second, with the relation:

$$Err = \frac{\Sigma_{i=1}^{100} \frac{|q_s - q_e|}{q_e}}{100}.$$

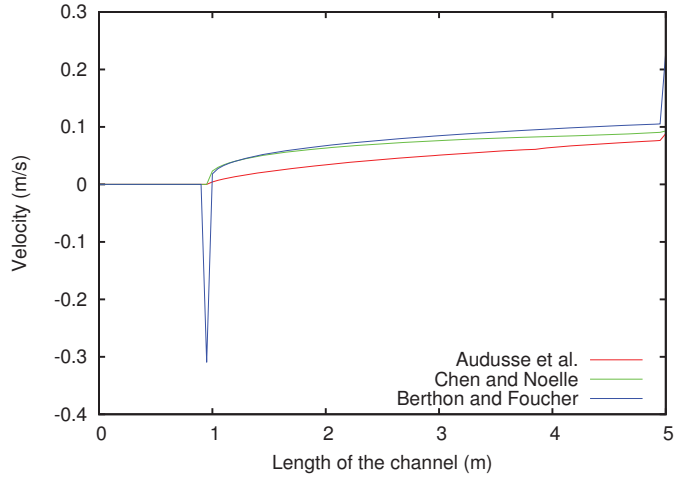

Fig. 5: Velocities (m/s) along the channel depending on the chosen scheme for the 5% slope simulation

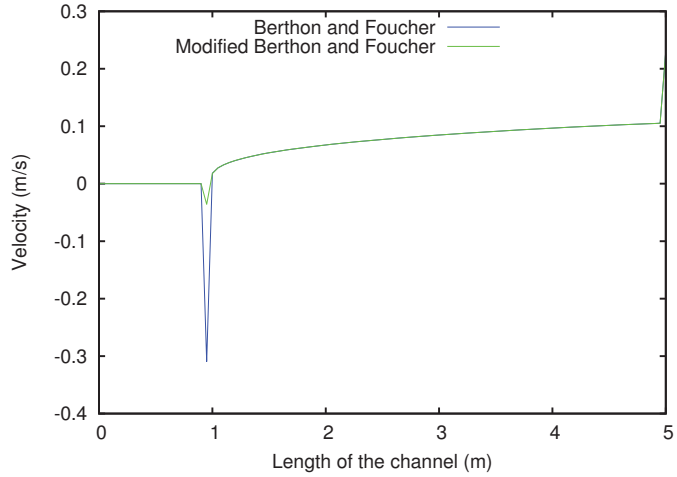

Fig. 6: Velocities (m/s) along the channel, effect of the correction on the Berthon and Foucher scheme for the 5% slope simulation

TABLE I: Relative error (%) of each scheme for the rise of the hydrograph and the constant value

Slope \ Scheme	Audusse *et al.*	Chen and Noelle	Berthon and Foucher
1%	7.97	8.86	5.88
5%	12.3	4.43	3.90
50%	24.7	1.02	2.71

The Berthon and Foucher's scheme [3] is the more efficient for the gentlest slopes (1% and 5%) while the Chen and Noelle's scheme [7] is more accurate for the steepest slope. Concerning the Audusse *et al.* scheme [1], it is more precise than the Chen and Noelle's scheme for the 1% slope, then, as it is shown in figure 2, for the 5% and 50% slopes, the results are far from the analytical solution.

Thus, we choose the Chen and Noelle's [7] hydrostatic reconstruction and the Berthon an Foucher's scheme [3] to test the tracers advection schemes and to couple the model with SISYPHE because of the slope limitation with the Audusse *et al.* [1] technique.

TABLE II: Concentration (g/l) of polluant for each scheme at one point at the outlet of the domain

Slope \ Scheme	LIPS [15]		ERIA [14]	
	Chen [7]	Berthon [3]	Chen [7]	Berthon [3]
1%	0.967	0.998	0.973	0.998
5%	0.970	0.999	0.970	0.999
50%	0.995	1.000	0.995	1.000

B. Polluant transfers

The objective here, is to ensure that these transport schemes can be used with the two new hydraulic finite volume schemes. A source term value of 1 g/l is fixed at one given point of the mesh, on the upstream part of the channel. The concentration at the central point of the outlet is measured. The table II gives the results of the concentration at the outlet for each scheme.

The results are similar, except for the 1% slope simulation where the ERIA scheme is more efficient. This scheme is chosen to solve the advection of the suspended sediment transport.

C. Erosion generation

1) Erosion without bottom modification: To simulate the erosion on the test case, we focus on the 5% and 50% slope because the maximal bed shear stress of the 1% simulation does not allow to have significant results. For every simulation, the erosion is homogeneous across the flow and is growing along the channel. Figure 7 shows the evolution of the bottom at the end of the simulations. On the 5% slope simulations, there is less erosion with the Chen and Noelle's scheme [7] than with the Berthon and Foucher's scheme [3], which is coherent with lag seen in figure 3. Concerning the 50% slopes, the erosion is similar for each scheme and the downstream boundary condition causes a deposition which is more important with the Berthon and Foucher's scheme [3]. Figure 8 shows the volumic concentration along the channel at the end of a 100 s simulation. We can observe that the concentration is lower for the Chen and Noelle's method [7] for the 5% slope which follows the results of the bottom evolution (figure 7). Concerning the 50% slope, the concentration profiles are similar. Some oscillations appear downstream in the Chen and Noelle's signal.

2) Erosion with topographical perturbation: Laboratory experiments ([2], [18]) have shown that rainfall in a straight channel could create a rill network due to erosion. This network depends on the spatial distribution and properties of the soil at the initial state. In our theoritical model, the soil is perfectly uniform at the initial state and the governing equations are solved to give exactly the same results along a cross section of the channel. To create a rill network, a perturbation of the soil at the initial state is introduced by adding to the topography a random number from a uniform law at each node of the mesh. The random number is drawn in

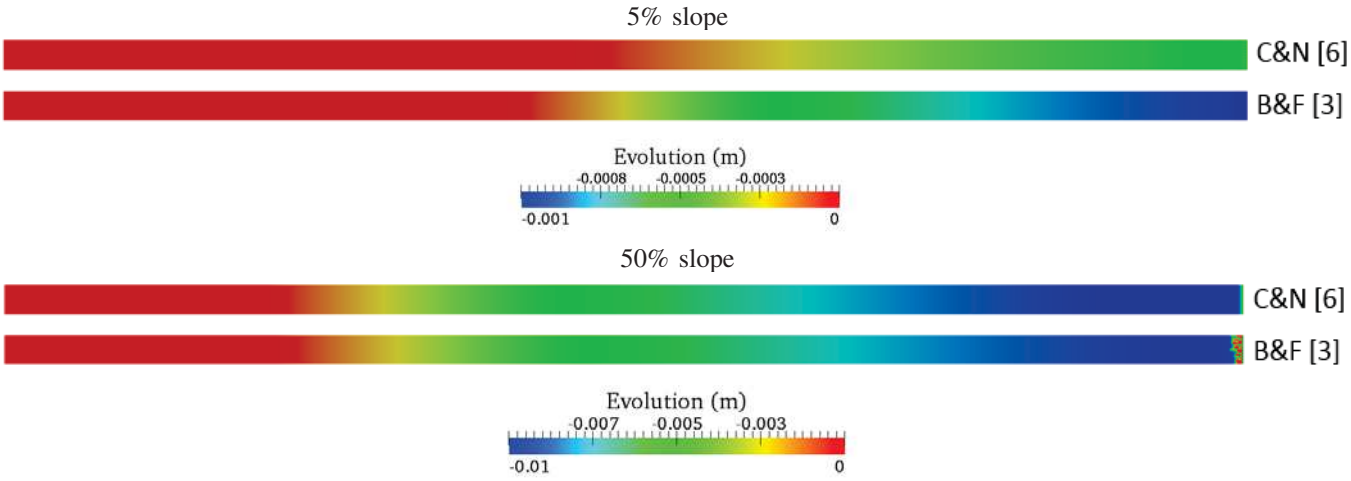

Fig. 7: Evolution of the bottom after 100 s of simulation with the two finite volume schemes and the 5% and 50% slopes

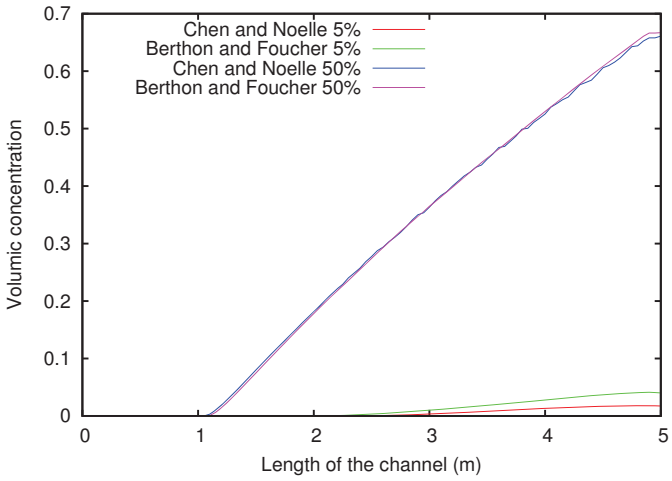

Fig. 8: Volumic concentration along the channel after 100 s of simulation with the two finite volume schemes and the 5% and 50% slopes

different intervals which characterize the size of the topographical perturbation. The sizes are 10^{-2} m, 10^{-3} m, 10^{-4} m and 10^{-5} m respectively defined by randomly drawing values from intervals of $[-10^{-2}; 10^{-2}]$, $[-10^{-3}; 10^{-3}]$, $[-10^{-4}; 10^{-4}]$ and $[-10^{-5}; 10^{-5}]$. Figure 9 illustrates the bottom elevation at the intial state for each size of the perturbation. For these simulations, we focus on the 5% slope case because the size of the distribution susceptible to generate rill erosion changes with the 50% slope.

Figure 10 presents the form of the erosion after 100 s of simulation depending on the range of the random number draw. For a 10^{-5} m and 10^{-4} m height of the perturbation, the bottom is smoothed whatever the hydraulic scheme, but the smoothing is more visible with the Berthon and Foucher's scheme [3], especially for the 10^{-4} m perturbation. For a 10^{-3} m size of the perturbation, a rill network is created, but the rills are wider with the Berthon and Foucher's scheme. For the higher height of the perturbation, we can see local erosion at certain points because the flow is blocked by the topographical pertubation and accumulates. For the Berthon and Foucher's scheme [3], local erosion is observed almost everywhere in the domain. This is due to the difficulty to treat the dry cells caused by the added topography. This highlights the difficulty of this scheme to handle wet/dry transition, even with the modification presented in III-A.

IV. Discussion

The hydrostatic reconstruction of Audusse *et al.* [1] can be a good choice for modelling hydraulic transfers over a watershed complex topography because of its properties. The positivity preserving and well-balanced properties, as well as its ability to deal with dry zones are crucial. The limitation of this technique, exhibited in figure 2, is a well-known problem. Indeed, [11] highlighted that for certain combinations of mesh size, slope and water height, the velocities are underestimated, in particular when $h < \Delta z$, with Δz the bottom difference between two neighboring points. This problem can be solved with a mesh refinement in a way to be always in the case $h > \Delta z$, but this is very expensive in term of computational time, especially with a view to model erosion on an entire watershed.

The development of the Chen and Noelle's [7] hydrostatic reconstruction method allows to overcome this problem. This technique consists of modifying the classical hydrostatic reconstruction when $h < \Delta z$, to take the full slope effect into account, while maintaining all the good properties of the scheme. Nevertheless, this modification causes problem when $\Delta z \approx h$ where the hydraulic values are not well calculated. For an application to a watershed case, this case is often oberved, for instance in the transition from plot runoff to river flow.

Analysis of the volumic concentration profiles confirms the diagnosis performed in the hydraulic part. Indeed, the 5% slope case is coherent with the underestimation of the velocities observed in figure 3. The computed shear stress being proportional to the square velocity, the difference between the concentration profile with the two schemes is even bigger

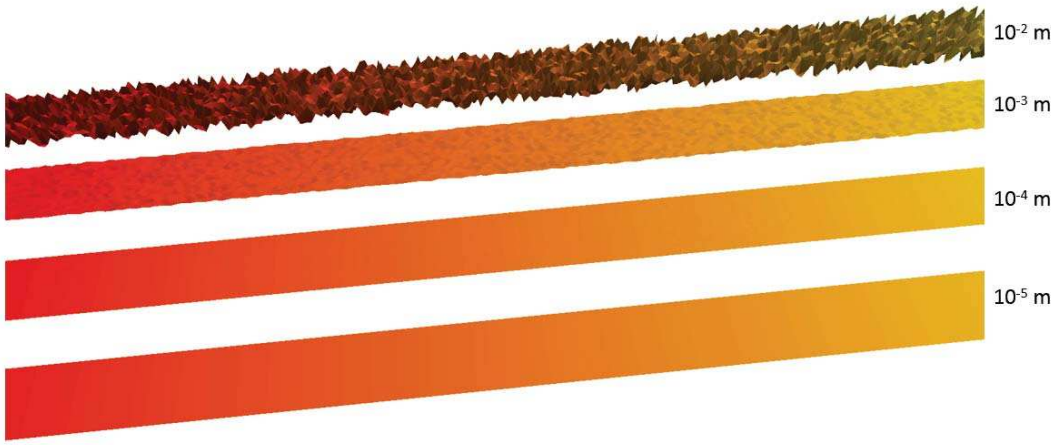

Fig. 9: 3D view of the initial bottom elevation in function of the range of the topographical perturbation

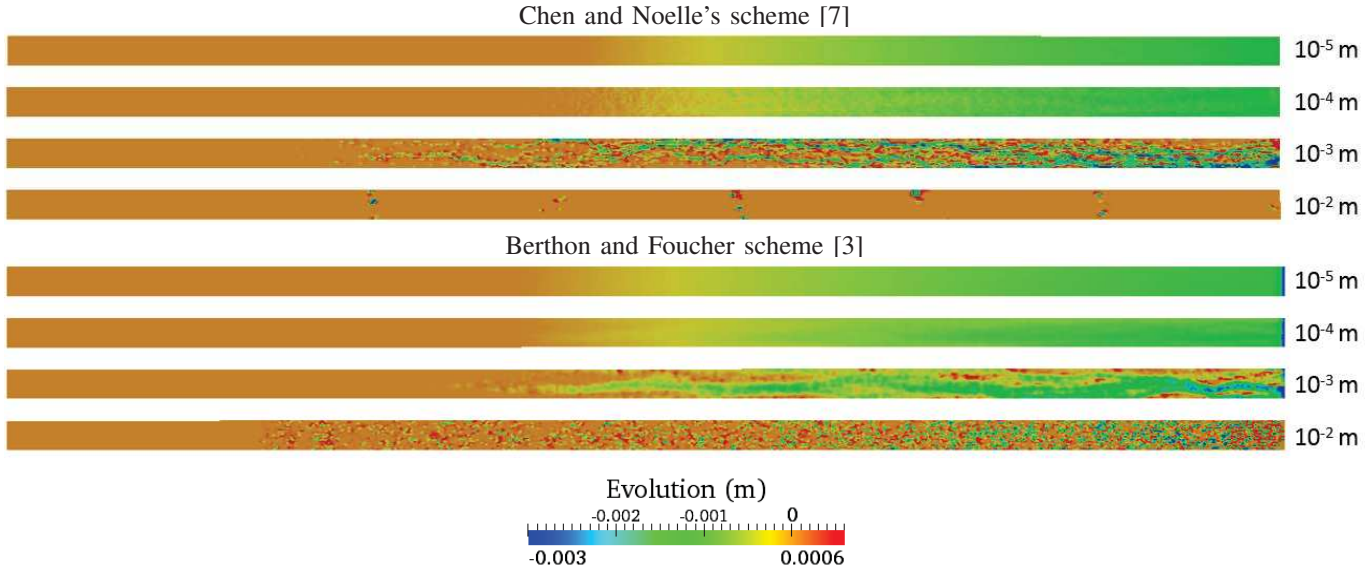

Fig. 10: Rills formation as a function of the range of the topographical perturbation, showing evolution of the bottom after 100 s of simulation

with a threshold law as the one used. Concerning the 50% slope simulation, the oscillation with the Chen and Noelle's technique [7] is due to the topographic difference created by the erosion. Indeed, the transport capacity of the flow is more important in this case so the bed evolution is faster and more susceptible to get close to the situation where $\Delta z = h$.

The Berthon and Foucher's scheme [3] presents issues at the wet/dry interface. These problems can be limited by using the Chen and Noelle's scheme [7] between a wet and a dry cell, but the equilibrium of the scheme is no more respected. In figure 10, for the highest magnitude of the topographical perturbation, these problems explain why the highest local erosion is simulated with this scheme. Its difficulty to deal with dry zones is an obstacle to its use for an application in watershed erosion. However, some treatment exists for this kind of problem (see [19]) but still needs to be adapted to this scheme.

V. Conclusion

The TELEMAC-SISYPHE hydrosedimentary computation code is adapted to river simulations. To extend the use to a watershed scale, a simple test case of runoff has been defined.

After highlighting the limits of the hydrostatic reconstruction present in the finite volume resolution for hydraulic computation (Audusse *et al.* [1]), two new schemes have been tested and have shown their efficiency in this test case (Chen and Noelle [7] and Berthon and Foucher [3]). The Chen and Noelle's hydrostatic reconstruction method is recommended as it is a good compromise between accuracy and robustness, has positivity preserving and well-balanced properties and is capable of handling the dry zones.

The advection schemes for passive tracer LIPS [15] and ERIA [14] give satisfactory results. When erosion is generated by SISYPHE on a smoothed bottom, the erosion is

homogeneous and the evolution of the bottom follows the hydraulic results. To generate rill erosion, a perturbation has been added to the bottom toopography. These configurations give very different results for these two schemes, and highlight the importance of the robustness of the Chen and Noelle's scheme.

As a perspective, there are still some ways to improve the code on this test case like adapt the treatment of the wet/dry interface with the Berthon and Foucher's [3] scheme or improve the Chen and Noelle's [7] method. Another scheme will be tested in future work: the Bouchut and Morales scheme [4] based on subsonic reconstruction. Then, these new methods will be confronted to real cases, thanks to data provided by the Draix-Bleone observatory [17]. The scale effects and the transition between hillslopes runoff and river flow will also be studied.

ACKNOWLEDGMENT

The authors would like to thank L. Staily for the help in this work.

REFERENCES

[1] E. Audusse, F. Bouchut, M.-O. Bristeau, R. Klein, and B. Perthame, "A fast stable well-balanced scheme with hydrostatic reconstruction for shallow water flows", *SIAM Journal on Scientific Computing*, vol. 25, no. 6, pp. 2050-2065, 2004.

[2] C. Berger, M. Schulze, D. Rieke-Zapp, and F. Schlunegger, "Rill development and soil erosion: a laboratory study of slope and rainfall intensity", *Earth Surface Processes and Landforms*, 2010.

[3] C. Berthon and F. Foucher, "Efficient well-balanced hydrostatic upwind schemes for Shallow-Water equations", *Journal of Computational Physics*, vol. 231, pp. 4993-5015, 2012.

[4] F. Bouchut and T. Morales, "A subsonic-well-balanced reconstruction scheme for shallow water flows", *SIAM Journal on Numerical Analysis*, vol. 48, pp. 1733-1758, 2010.

[5] M. O. Bristeau and B. Coussin, "Boundary conditions for the Shallow Water equations solved by kinetic schemes", INRIA, Technical Report 4282, 2001.

[6] N. Chahinian, "Comparison of infiltration models to simulate flood events at the field scale", *Journal of Hydrology*, vol. 306, pp. 191-214, 2005.

[7] G. Chen and S. Noelle, "A new hydrostatic reconstruction scheme based on subcell reconstructions", submitted to *SIAM Journal on Numerical Analysis*, 2015.

[8] N. Claude, "Interactions entre végétation, processus hydro-sédimentaires et morphodynamique des cours d'eau : état de l'art et principes de modélisation", *Note EDF LNHE ref. H-P73-2014-05213-FR*, 2015.

[9] O. Delestre, "Simulation du ruissellement deau de pluie sur des surfaces agricoles", Ph.D. dissertation, Université d'Orléans, 2010.

[10] O. Delestre and F. James, "Simulation of rainfall events and overland flow", *Proceedings of X International Conference Zaragoza-Pau on Applied Mathematics and Statistics, Jaca, Spain, september 2008, Monografas Matemticas Garca de Galdeano*, 2009.

[11] O. Delestre, S. Cordier, F. Darboux, and F. James, "A limitation of the hydrostatic reconstruction technique for shallow water equations", *Compte Rendu de l'Académie des Sciences, Série I*, vol. 350, pp. 677-681, 2012.

[12] F. R. Fiedler and J. A. Ramirez, "A numerical method for simulating discontinuous shallow flow over an infiltrating surface", *International Journal for Numerical Methods in Fluids*, vol. 32, pp. 219-240, 2000.

[13] J. M. Greenberg and A.-Y. Leroux, "A well-balanced scheme for the numerical processing of source terms in hyperbolic equations", *SIAM Journal on Numerical Analysis*, vol. 33, no. 1, pp. 1-16, 1996.

[14] J.-M. Hervouet, "Latest news on distributive schemes and dry zones: the ERIA scheme", in *Telemac-Mascaret User Conference*, 2016.

[15] J.-M. Hervouet, S. Pavan, and R. Ata, "Distributive advection schemes and dry zones, new solutions", in *Telemac-Mascaret User Conference*, 2015.

[16] G. Kirstetter, J. Hu, O. Delestre, F. Darboux, P.-Y. Lagre, S. Popinet, J. M. Fullana, and C. Josserand, "Modeling rain-driven overland flow: empirical versus analytical friction terms in the shallow water approximation", *Journal of Hydrology*, vol. 536, pp. 1-9, 2016.

[17] C. Le Bouteiller, S. Klotz, F. Libault, M. Estèves, "Observatoire hydrosdimentaire de montagne Draix-Blone", http://dx.doi.org/10.17180/OBS.DRAIX, Irstea, 2015.

[18] K. Michaelides, I. Ibraim, G. Nord, and M. Esteves, "Tracing sediment redistribution across a break in slope using rare earth elements", *Earth Surface Processes and Landforms*, vol. 35, pp. 575-587, 2010.

[19] V. Michel-Dansac, C. Berthon, S. Clain and F. Foucher, "A well-balanced scheme for the Shallow-Water equations with topography", *hal-01201825*, 2015.

[20] T. Takahashi, "Debris flow: Mechanics, Prediction and Countermeasures", Taylor & Francis, 2007.

[21] P. Tassi and C. Villaret, "Sisyphe v6.3 Users Manual", *Note EDF LNHE ref. H-P74-2012-02004-EN*, 2014.

[22] E. F. Toro, "Riemann Solvers and Numerical Methods for Fluid Dynamics", Springer, 2009.

[23] E. F. Toro, M. Spruce, and W. Speares, "Restoration of the contact surface in the HLL-Riemann solver", *Shock Waves*, vol. 4, pp. 25-34, 1994.